

## CHARACTERISTICS AND OPTICAL PROPERTIES OF Fe<sup>3+</sup> DOPED SiO<sub>2</sub>/TiO<sub>2</sub> THIN FILMS PREPARED BY THE SOL-GEL DIP-COATING METHOD

Dang Mau Chien, Le Duy Dam, Nguyen Thi Thanh Tam and Dang Thi My Dung

Laboratory for Nanotechnology, Vietnam National University, Ho Chi Minh City

(Manuscript Received on April 5<sup>th</sup>, 2012, Manuscript Revised May 15<sup>th</sup>, 2013)

**ABSTRACT:** In this study, we have successfully synthesized Fe<sup>3+</sup> doped SiO<sub>2</sub>/TiO<sub>2</sub> thin films on glass substrates using the sol-gel dip-coating method. After synthesizing, the samples were annealed at 500<sup>o</sup>C in the air for 1 hour. The characteristics and optical properties of Fe<sup>3+</sup> doped SiO<sub>2</sub>/TiO<sub>2</sub> films were then investigated by X-ray diffraction (XRD), ultraviolet-visible spectroscopy (UV-vis) and Fourier transform infrared spectroscopy (FT-IR). An antifogging ability of the glass substrates coated with the fabricated film is investigated and explained by a water contact angle under visible-light. The analyzed results also show that the crystalline phase of TiO<sub>2</sub> thin films comprised only the anatase TiO<sub>2</sub>, but the crystalline size decreased from 8.8 to 5.9 nm. We also observed that the absorption edge of Fe<sup>3+</sup>-doped SiO<sub>2</sub>/TiO<sub>2</sub> thin films shifted towards longer wavelengths (i.e. red shifted) from 371.7nm to 409.2 nm when the Fe<sup>3+</sup>-doped concentration increased from 0 to 1 % mol.

### 1. INTRODUCTION

Titanium dioxide (TiO<sub>2</sub>) is a nontoxic material and has been applied in environmental treatments such as water and air purification, water disinfection and sterilization because of

Its unique properties such as strong photocatalytic activity and chemical stability [1]. However, the major limitations of TiO<sub>2</sub> are the absorption region in the UV light (about 4% - 5% of solar energy) and fast recombination of hole–electron pairs within nanoseconds. To propose using TiO<sub>2</sub> to the coating on the ceramic tiles and glass to make intelligent materials was being able self-cleaning and antibacterial. In our previous papers [2, 3] we have reported the influence of doping SiO<sub>2</sub> was exhibited higher photocatalytic activity than pure TiO<sub>2</sub>. This

could be explained by the addition of SiO<sub>2</sub> into TiO<sub>2</sub> retarding or inhibiting the crystallization of anatase phase. A contact angle of SiO<sub>2</sub>/TiO<sub>2</sub> thin films with 15 mol % SiO<sub>2</sub> concentrations is less than 2<sup>o</sup> and these films can maintain a super-hydrophilic property for a long time in dark conditions, thus exhibiting excellent antifogging capabilities [3]. In this paper we focused on improving the photocatalytic activity of SiO<sub>2</sub>/TiO<sub>2</sub> films in the visible light region. Transition metal ions and noble metals have been employed to dope into TiO<sub>2</sub> in order to induce a red shift in the absorption band [4, 5]. Among these metals, iron has been considered to be an appropriate candidate owing to its radius of Fe<sup>3+</sup> (0.64 Å) is similar to that of Ti<sup>4+</sup> (0.68 Å), therefore, it can be inferred that Fe<sup>3+</sup> ions might easily incorporate

into the crystal lattice of TiO<sub>2</sub>. Furthermore, Fe<sup>3+</sup> ions can play a role as e<sup>-</sup>/h<sup>+</sup> pair traps because the energy level of Fe<sup>2+</sup>/Fe<sup>3+</sup> lies close to that of Ti<sup>3+</sup>/Ti<sup>4+</sup>, favoring the separation of the photo-generated e<sup>-</sup>/h<sup>+</sup> pair, and consequently reducing e<sup>-</sup>/h<sup>+</sup> pair recombination rate [6,10].

**2. EXPERIMENTAL**

The following chemicals were used: Tetra-isopropyl Ortho-titanate Ti (OC<sub>3</sub>H<sub>7</sub>)<sub>4</sub> (TIPOT-Merk), Tetra-ethoxyortho-silicate Si(OC<sub>2</sub>H<sub>5</sub>)<sub>4</sub> (TEOS-Merck), Ethanol C<sub>2</sub>H<sub>5</sub>-OH (Merck), HCl-Hydrochloric acid (China), Iron(III)Nitrate Fe(NO<sub>3</sub>)<sub>3</sub>.9H<sub>2</sub>O (Merck), DI water. The synthesis process of the Fe-doped SiO<sub>2</sub>/TiO<sub>2</sub> solution is shown in Figure 1.

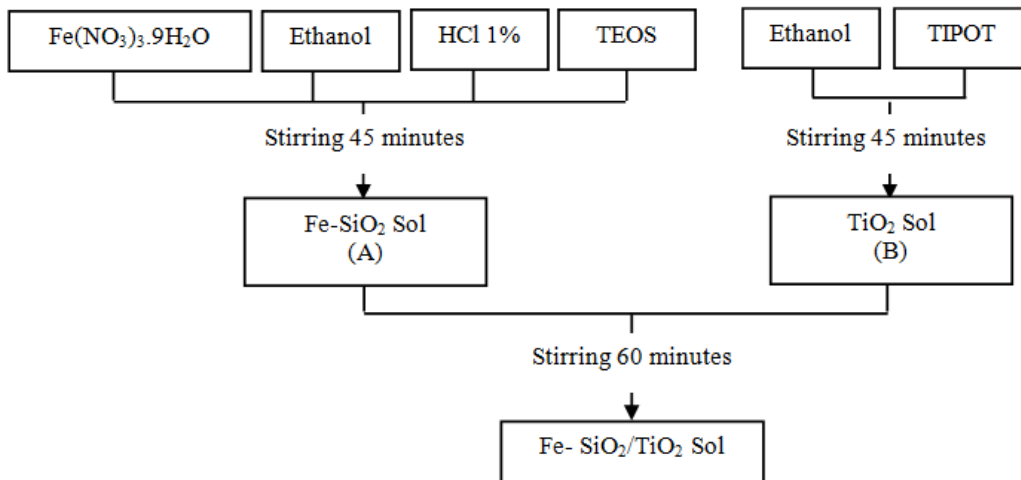


**Figure 1.** The synthesis process of the Fe<sup>3+</sup>-doped SiO<sub>2</sub>/TiO<sub>2</sub> solution prepared soil-gel method

The volume of H<sub>2</sub>O containing 1 wt% HCl can be determined by the formula:

$$R = \frac{n_{H_2O}}{n_{TiO_2} + n_{SiO_2}} = \frac{8}{3} \quad (1)$$

In this report, we synthesized the Fe<sup>3+</sup>-doped SiO<sub>2</sub>/TiO<sub>2</sub> coating solution with various Fe/(SiO<sub>2</sub>+TiO<sub>2</sub>) molar ratios: from 0 to 1%. The Fe<sup>3+</sup>-doped SiO<sub>2</sub>/TiO<sub>2</sub> thin films were deposited on glass substrates by a dip coating process at room temperature. Glass slides with dimensions of (26x76) mm<sup>2</sup> were used as substrates. Before the deposition, the substrates were ultrasonically cleaned in dilute HCl,

acetone and absolute ethanol for 30 min, respectively. Finally, they were thoroughly rinsed with DI water.

The substrates were immersed into as-prepared Fe-doped SiO<sub>2</sub>/TiO<sub>2</sub> sol for 30 seconds. The substrates were then withdrawn from the sol with velocity 5 mm/s. If coating two times or more, each layer would be dried between two successive coatings at 230<sup>o</sup>C for 5 min before the next coating was implemented. Afterward, the substrates were annealed at 500<sup>o</sup>C for 1 h. X-ray diffraction (XRD) patterns of these powder samples were

measured with a diffractometer (D8 Advance). An atomic force microscope (AFM-Electronica S.L) was used to investigate the crystallization and surface structure. Synthesized samples were also studied using UV-VIS absorption spectra with UV-VIS equipment (Cary 100 Conc)-spectrophotometer in a wavelength range from 200 to 800 nm, and Fourier transform infrared spectroscopy (FTIR) TensorTM 37 (Bruker) in the range 400-4000  $\text{cm}^{-1}$  by the KBr pellet technique.

### 3. RESULTS AND DISCUSSION

#### 3.1. UV-vis results

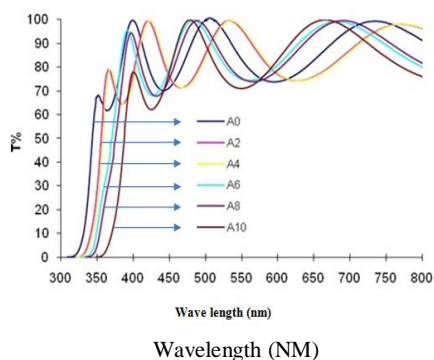


**Figure 2.** The UV-vis spectra of  $\text{SiO}_2/\text{TiO}_2$  thin films with different Fe-doped concentrations in the wavelength range of 300-800 nm.

The ultraviolet-visible (UV-Vis) spectra of  $\text{SiO}_2/\text{TiO}_2$  thin films with different  $\text{Fe}^{3+}$ -doped concentrations in the wavelength range of 300–800 nm are illustrated in Figure 2. It reveals that the transmittance of  $\text{SiO}_2/\text{TiO}_2$  thin film without  $\text{Fe}^{3+}$  doping has an abrupt decrease when wavelengths are below 350 nm. This indicates the absorption edge near 350 nm

and reach almost near zero at about 300 nm. The transmittance quickly decreases when below 350 nm due to the absorption of light caused by the excitation of electrons from the valence band to the conduction band of  $\text{TiO}_2$ . The absorption edge shifted towards longer wavelengths (i.e. red shifted) from 350 to 410 nm with the  $\text{Fe}^{3+}$ -doped concentration increasing from 0 to 1% mol. Red shift associated with the presence of dopants can be attributed to a charge transfer transition between the iron d electrons and the  $\text{TiO}_2$  conduction or valence band [7], [11]. With this result, this material system can be applied to manufacturing photo-catalyst  $\text{Fe}^{3+}$ -doped  $\text{SiO}_2/\text{TiO}_2$  nano materials in the visible light range.

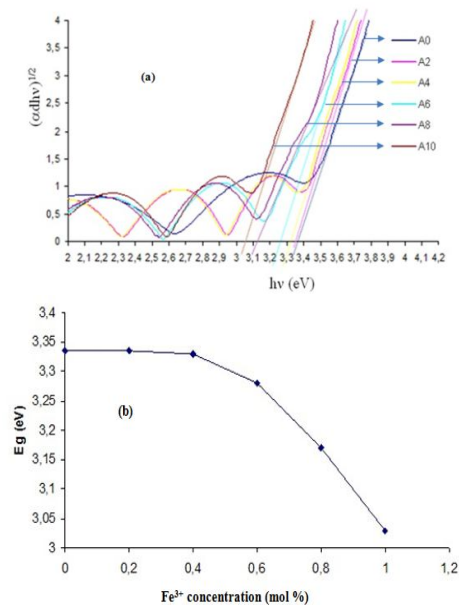


**Figure 3.** (a) The plot of  $(\alpha h\nu)^{1/2}$  vs.  $h\nu$ , (b) The relationship between band-gap energy and  $\text{Fe}^{3+}$ -doped concentration.

Figure 3 (a) illustrates the plot of  $(\alpha\text{d}h\nu)^{1/2}$  vs.  $h\nu$  for the  $\text{TiO}_2$  thin films with various  $\text{Fe}^{3+}$  contents. From the intersection of the extrapolation of each curve in Figure 3(a) and  $h\nu$  axis gives the band-gap energy of  $\text{TiO}_2$  thin films with different  $\text{Fe}^{3+}$  doping concentrations. The relationship between the band-gap energy and the  $\text{Fe}^{3+}$  content, for all  $\text{SiO}_2/\text{TiO}_2$  thin films, are shown in Figure 3(b). It reveals that the band-gap energy decreases when the  $\text{Fe}^{3+}$  content increases. The band-gap energy of  $\text{SiO}_2/\text{TiO}_2$  thin film without  $\text{Fe}^{3+}$  doping is 3.33 eV and the band-gap energy of  $\text{SiO}_2/\text{TiO}_2$  thin film doping with 1 mol%  $\text{Fe}^{3+}$  has been identified to be 3.03 eV. Since localized 3d orbitals of Ti constitute the conduction band of  $\text{TiO}_2$ , doping  $\text{Fe}^{3+}$  to the  $\text{TiO}_2$  lattice influence, the conduction band by admixing  $\text{Fe}^{3+}$  3d orbitals [8]. Thus, the conduction band is shifted towards the lower energy and a systematic decrease in the valence band-conduction band occurs with an increasing concentration of  $\text{Fe}^{3+}$  in  $\text{TiO}_2$  lattice or matrix.

**Table 2.** From the value of  $E_g$  (eV) and  $\lambda_{\text{ht}}$

Samples	$E_g$ (eV)	$\lambda_{\text{ht}}$ (m)
A0	3.336	371.7
A2	3.335	371.8
A4	3.331	372.2
A6	3.28	378.0
A8	3.17	391.2
A10	3.03	409.2

### 3.2. X-ray diffraction Measurements

XRD patterns for undoped and various  $\text{Fe}^{3+}$ -doped  $\text{SiO}_2/\text{TiO}_2$  powders calcined at  $500^\circ\text{C}$  for 1h are shown in Figure 4. It is identified that all the diffraction peaks are ascribed to the anatase  $\text{TiO}_2$  for undoped  $\text{Fe}^{3+}$  powders as illustrated in Figure 4 (A0). The XRD patterns of the  $\text{SiO}_2/\text{TiO}_2$  powders with an  $\text{Fe}^{3+}$ -doping amount increasing from 0 to 1mol % are demonstrated in Figure 4(A2–A10), respectively. It has been registered that all the diffraction peaks in Figure 4(A2–A10) also belong to the anatase  $\text{TiO}_2$ , and no other phase can be detected. Moreover, the result of Figure 4 also reveals that the intensity of diffraction peaks decreases with an increasing  $\text{Fe}^{3+}$ -doped concentration. This phenomenon caused by the  $\text{Fe}^{3+}$ -doped can inhibit the crystallization of anatase  $\text{TiO}_2$  [11].

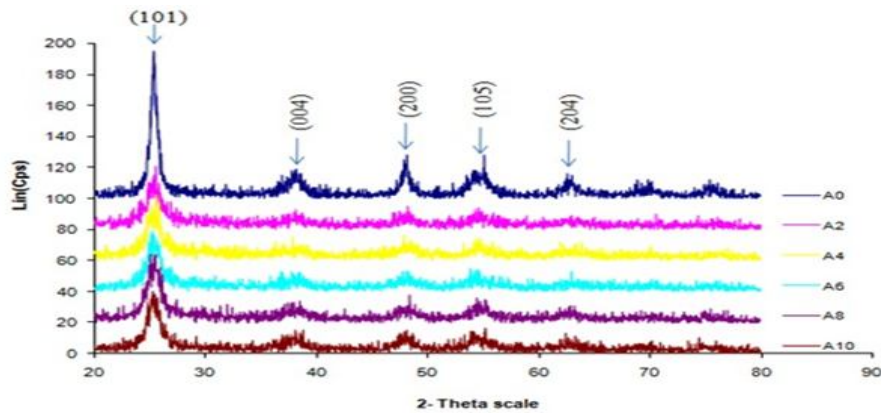


**Figure 4.** XRD patterns for undoped and various Fe<sup>3+</sup>-doped TiO<sub>2</sub> thin films after calcining at 500<sup>0</sup>C for 1h.

Moreover, in this study, although the Fe<sup>3+</sup>-doped concentration attained 1 mol %, the iron oxides or Fe<sub>x</sub>TiO<sub>y</sub> are not identified in the XRD patterns. The average crystallite size of the TiO<sub>2</sub> powders with various Fe<sup>3+</sup>-doped concentrations calcined at 500<sup>0</sup>C for 1h are determined, by the Scherrer's equation, as follows:

$$D_{hkl} = \frac{0.89\lambda}{\beta \cos\theta} \quad (2)$$

Where D<sub>hkl</sub> denotes the average crystallite size of the TiO<sub>2</sub> powders with various Fe<sup>3+</sup>-doped concentrations, λ= 0.15405 nm is the X-ray wavelength of Cu Kα, β is the full width of the peak measured at half maximum intensity and θ is the Bragg's angle of the peak. The effects of the Fe<sup>3+</sup>-doped concentration on the crystallite size of TiO<sub>2</sub> powders calcined at 500<sup>0</sup>C for 1h are demonstrated in Figure 5.

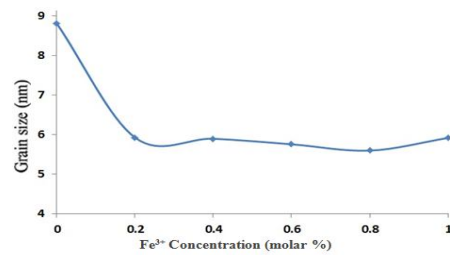


**Figure 5.** Effect of Fe<sup>3+</sup>-doped concentrated on the crystalline size of TiO<sub>2</sub> thin films.

It reveals that the size of TiO<sub>2</sub> powder decreases from 8.8 to 5.59 nm when the Fe<sup>3+</sup>-doped concentration increases from 0 to 0.8 mol%. The Fe<sup>3+</sup>-doped has an effect on the crystallization of TiO<sub>2</sub> [9]. The larger the amount of Fe<sup>3+</sup>-doping, the wider the width of the diffraction peaks, the worse the crystallization, and the smaller the grain size of TiO<sub>2</sub> powders.

### 3.3. Raman Measurement

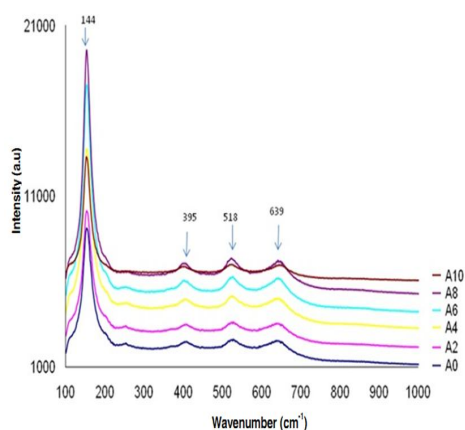


**Figure 6.** Raman spectrum of powder samples A0, A2, A4, A6, A8, A10.

Figure 6 shows the Raman spectra of different samples. Raman peak at about  $144\text{ cm}^{-1}$  is observed for all the samples, which is attributed to the main  $E_g$  anatase vibration mode. Moreover, vibration peaks at  $395\text{ cm}^{-1}$ ,  $518\text{ cm}^{-1}$  and  $639\text{ cm}^{-1}$  are presented in the spectra for all samples, which indicate that anatase  $\text{TiO}_2$  crystalline are the predominant species. Furthermore, there is no peak attributed to the iron oxide observed, which is consistent with the results of XRD patterns.

### 3.4. AFM result images

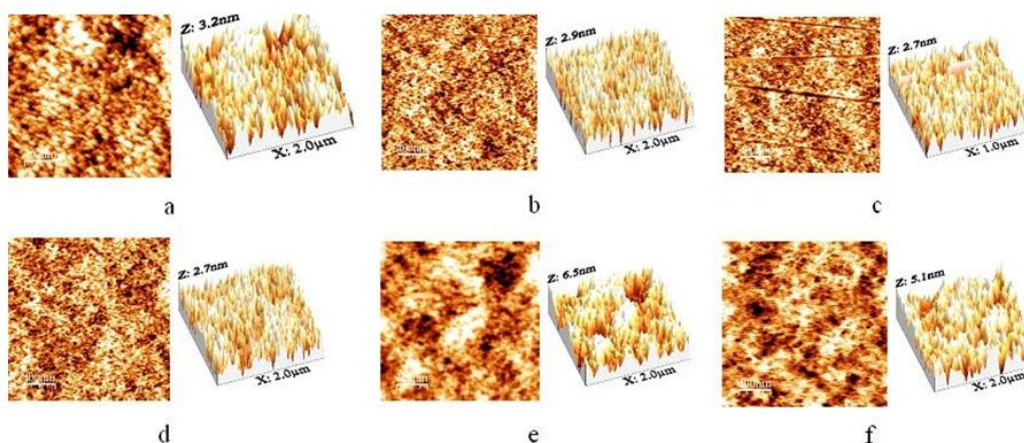


**Figure 7.** AFM images of film: a. A0 with RMS = 0.7565 nm; b. A2 with RMS = 0.6772 nm; c. A4 with RMS = 0.5812nm; d. A6 with RMS=0.6526nm; e. A8 with RMS=1.5891nm; f. A10 with RMS = 1.2298nm.

The atomic force microscopy images were taken in order to study the morphology of the  $\text{Fe}^{3+}$ -doped  $\text{SiO}_2/\text{TiO}_2$  thin films. The AFM images in Figure 7 indicate that the particle size and film roughness increased with the increase of  $\text{Fe}^{3+}$ . The surface roughness (RMS) increased from 0.7565 nm to 1.5891 nm with the addition of  $\text{Fe}^{3+}$  from 0 mol% to 0.8 mol%

respectively. The surface roughness increases this mean that, it is favorable to a photocatalytic reaction by enhancing the contact surface area between  $\text{Fe}^{3+}$ -doped  $\text{SiO}_2/\text{TiO}_2$  films and organic pollutants. The AFM images of samples showing RMS A8 is the largest, therefore the roughness of film A8 are the highest.

### 3.5. Visible photocatalytic activity

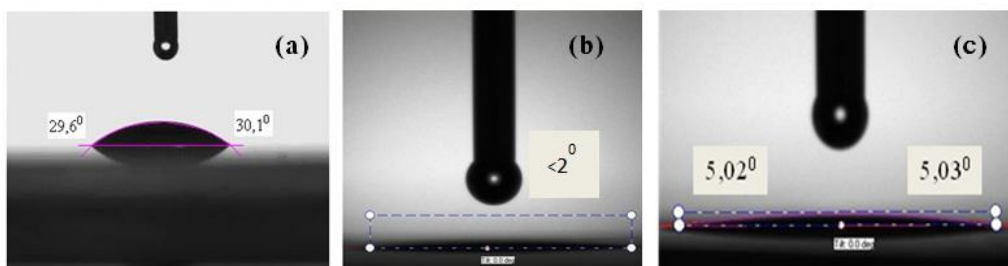


**Figure 8.** The contact angle of water on the normal glass substrate (a), on A8 film (b) and on A8 film stored 1 day in a dark environment (c).

Figure 8 shows that the dependence of photo-induced changes in the water contact angle of  $\text{Fe}^{3+}$ -doped  $\text{SiO}_2/\text{TiO}_2$  thin film with  $\text{Fe}^{3+}$  0.8 mol % coated on glass, which were irradiated under visible-light after 2 hours and then kept 1 day in a dark environment. The hydrophilic ability of the sample may be explained by the contact angle of water on the surface. The super-hydrophilic property of the surface allows water to spread completely across the surface rather than remaining as droplets. The observed result means that  $\text{Fe}^{3+}$ -doped  $\text{SiO}_2/\text{TiO}_2$  film coated glass is a good material for antifogging and self-cleaning purposes.

Moreover, Figure 8(b) shows that, the contact angle of water on the  $\text{Fe}^{3+}$ -doped  $\text{SiO}_2/\text{TiO}_2$  film coated sample was very low ( $< 2^{\circ}$ ), while higher values of water contact angle resulted when water was deposited on normal glass substrates. In addition, after storing 1 day in a dark environment, the contact angle of water on  $\text{Fe}^{3+}$ -doped  $\text{SiO}_2/\text{TiO}_2$  film coated glass slowly increased to about  $5^{\circ}$  (Figure 8 (c)). This result means that the coated sample could maintain the super-hydrophilic capability for a long time in a dark environment.

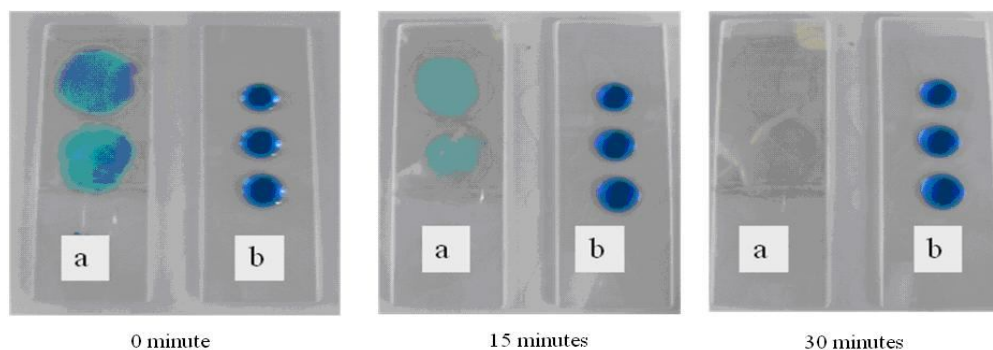


**Figure 9.** Photocatalysis decoloration of MB with A8 film/glass (a), and normal glass substrate (b)

Finally, we qualitatively analyze the photocatalysis property of  $\text{Fe}^{3+}$ -doped  $\text{SiO}_2/\text{TiO}_2$  film on glass substrates by decoloration of MB. Figure 9 shows the photocatalysis decoloration of MB with A8-coated glass substrate. It can be seen that the concentration of MB on the experimental substrate decreased about 50% over a period of about 15 min and almost no MB was detected after a period of 30 min.

#### 4. CONCLUSIONS

The  $\text{SiO}_2/\text{TiO}_2$  films doped with different  $\text{Fe}^{3+}$  concentration have been prepared by a simple sol-gel method. The solutions have high

stability and may be utilized for mass production. The absorption edge of thin films shifted towards longer wavelengths from 371.7 to 409.2 nm with increasing concentrations of  $\text{Fe}^{3+}$ . The result shows that, the optimum concentration of  $\text{Fe}^{3+}$  is 0.8 % mol at  $500^\circ\text{C}$  temperature of substrates. It was found that doped  $\text{Fe}^{3+}$  increases the photosensitivity of nano  $\text{TiO}_2$  with rather high retention time in characteristics. The as-prepared material can be used to manufacture  $\text{TiO}_2$  operating in the region of visible light.

### ĐẶC ĐIỂM VÀ TÍNH CHẤT QUANG CỦA MÀNG $\text{SiO}_2/\text{TiO}_2$ PHA TẠP $\text{Fe}^{3+}$ CHẾ TẠO BẰNG PHƯƠNG PHÁP PHỦ NHÚNG SOL – GEL

Đặng Mậu Chiến, Lê Duy Đảm, Nguyễn Thị Thanh Tâm, Đặng Thị Mỹ Dung

Phòng thí nghiệm Công nghệ Nano, ĐHQG-HCM

**TÓM TẮT:** Trong bài báo này, chúng tôi đã tổng hợp thành công màng  $\text{SiO}_2/\text{TiO}_2$  pha tạp  $\text{Fe}^{3+}$  trên đế thủy tinh sử dụng phương pháp phủ nhúng Sol-Gel. Màng sau khi chế tạo được nung ở  $500^\circ\text{C}$  trong không khí trong 1 giờ. Đặc điểm và tính chất quang của màng  $\text{SiO}_2/\text{TiO}_2$  pha tạp  $\text{Fe}^{3+}$  đã được khảo sát bằng nhiễu xạ tia X, quang phổ UV-Vis và quang phổ hồng ngoại (FT-IR). Khả năng chống đọng sương mờ trên kính có phủ màng  $\text{SiO}_2/\text{TiO}_2$  pha tạp  $\text{Fe}^{3+}$  đã được khảo sát và chứng minh bằng góc tiếp xúc của nước dưới ánh sáng khả kiến. Kết quả phân tích cũng chỉ ra rằng tinh thể  $\text{TiO}_2$  tạo là pha anatase và kích thước tinh thể giảm dần từ 8.8 đến 5.9 nm. Kết quả thu được cũng cho thấy bờ hấp thụ của màng  $\text{SiO}_2/\text{TiO}_2$  pha tạp  $\text{Fe}^{3+}$  dịch chuyển tới bước sóng dài hơn (dịch chuyển tới ánh sáng đỏ) từ 371nm tới 409.2 nm khi nồng độ tạp  $\text{Fe}^{3+}$  tăng lên từ 0 đến 1% mol.



**REFERENCES**

- [1]. Michael R. Hoffmann, Scot T. Martin, Wonyong. Choi, Detlef W. Bahnemann, Environmental Applications of Semiconductor Photocatalysis, *Chemical Reviews*, 95, 69-96 (1995)
- [2]. Dang Mau Chien, Nguyen Ngoc Viet, Nguyen Thi Kieu Van, Nguyen Thi Phuong Phong, Characteristics modification of TiO<sub>2</sub> thin films by doping with silica and alumina for self-cleaning application, *Journal of Experimental Nanoscience*, 4, 221-232 (2009).
- [3]. Dang Mau Chien, Nguyen Ngoc Viet, Nguyen Thi Kieu Van, Nguyen Thi Phuong Phong, SiO<sub>2</sub>-TiO<sub>2</sub> thin film and its photocatalyst properties, *Advances in Natural Sciences*, 10, 31 (2009).
- [4]. Thi My Dung Dang, Duy Dam Le, Vinh Thang Chau, Mau Chien Dang, Visible-light photocatalytic activity of N/SiO<sub>2</sub>-TiO<sub>2</sub> thin films on glass, *Adv. Nat. Sci: Nanosci. Nanotechnol.* 1 015004 (2010).
- [5]. Duy Dam Le, Thi My Dung Dang, Vinh Thang Chau, Mau Chien Dang, The fabrication of visible light responsive Ag-SiO<sub>2</sub> co-doped TiO<sub>2</sub> thin films by the sol-gel method, *Adv. Nat. Sci: Nanosci. Nanotechnol.* 1 015007 (2010).
- [6]. J. Zhu, W. Zhang, B. He, J. Zhang, M. Anpo, J. Huang, L. Zhang, Characterization of Fe-TiO<sub>2</sub> photocatalysts synthesized by hydrothermal method and their photocatalytic reactivity for photodegradation of XRG dye diluted in water, *J. Mol. Catal. A: Chem.*, 216, 35 (2004).
- [7]. D.H. Kim, H.S. Homg, S.J. Kim, J.S. Song, K.S. Lee, Photocatalytic behaviors and structural characterization of nanocrystalline Fe-doped TiO<sub>2</sub> synthesized by mechanical alloying, *J. Alloys Compounds*, 375, 259 (2004).
- [8]. M. Radecka, P. Pasierb, K. Zakrzewska, M. Rekas, Transport properties of (Sn,Ti)O<sub>2</sub> polycrystalline ceramics and thin films, *Solid State Ionics* 119, 43 (1999).
- [9]. M. Zhou, J. Yu, B. Cheng, H. Yu, Preparation and photocatalytic activity of Fe-doped mesoporous titanium dioxide nanocrystalline photocatalysts, *Mater. Chem. Phys.*, 93, 159 (2005)
- [10]. Kais Elghniji, Atef Atyaoui, Stefano Livraghi, Latifa Bousselmi, Elio Giamello, Mohamed Ksibi, Synthesis and characterization of Fe<sup>3+</sup> doped TiO<sub>2</sub> nanoparticles and films and their performance for photocurrent response under UV illumination, *Journal of Alloys and Compounds*, 541, 421 (2012).
- [11]. J. Ben Naceura, R.Mechiakha, F. Bousbih, R. Chtourou, Influences of the iron ion (Fe<sup>3+</sup>)-doping on structural and optical properties of nanocrystalline TiO<sub>2</sub> thin films prepared by sol-gel spin coating, *Applied Surface Science* 257 10699 (2011).